Influence of Activation Energy, Variable Viscosity, Partial Slip on MHD Mixed Convective Heat Transfer Flow of Nanofluid Past Stretching Surface with Newtonian Cooling

D. Chitti Babu, PhD
Principal, Govt. Degree College,
Seethanagaram, East Godavari (Dt.), A.P., India

ABSTRACT
An attempt has been made to explore the impact of Activation energy, Brownian motion, thermophoresis and the influence of changing viscosity and the current of Hall on hydro-magnetic free-convective flow, the transfer of energy and mass flow of a nanofluid across its stretched surface with Newtonian cooling and partial slip. The nonlinear in nature coupled mathematical equations regulating the flow were solved using the fifth-order Runge-Kutta-Fehlberg approach in conjunction with the firing technique. The impacts of different constants on the flow rates(f',g), temperature(θ), and nano-concentration(ϕ), as well as the local skin-friction($Cf_{x,z}$) coefficient, local Nusselt(Nu) and Sherwood(Sh) numbers are graphed and analysed. It is found that θ upsurges with increase in Nb, Nt, h1 and reduces with θr and Rd. Nanoparticle concentration decay with Rd ,θr and convective heat transfer constant (h1). Higher the activation energy (E1) bigger θ and smaller the nanoparticle concentration. Nu enhances with Nt, diminishes with Nb, θr and h1. Sh smaller with E1 and upsurges with δ.

Keywords
Stretching sheet, Newtonian cooling, Brownian Motion, Thermophoresis, variable viscosity, Activation energy.

1. INTRODUCTION

Activation energy which is an important concenpt related to a chemical kinetics is often studied under physical chemistry. In the year 1889, Swedish scientist, Svante Arrhenius used the term Activation Energy. Present improvements in the computation and understanding of a kinetic method's activation energy are explained. The direct estimation of the energy required to activate for an infinite cyclical timeframe from simulations at a single temperature, in specific, is currently addressed via statistical mechanics' fluctuation theory applied to kinetics.This opens up new options for active processes in situations when a typical Arrhenius analysis is not practicable. The strategies aid in the systematic deconstruction of activation energy into components associated with the system's many interactions and movements. These components can be understood using Tolman's understanding of activation energy. Researchers specifically give insight into how energy might be most efficiently injected in order to speed up a mechanism of specialty, promising significant new structural knowledge for future research.

The movement of fluid difficulties past a stretched sheet are significant in activities such as protrusion, there wire sketching, aluminium weaving, and hot rolling.Understanding the heat and the flow patterns of this procedure is critical for ensuring that the completed product satisfies the appropriate quality criteria. Numerous studies on heat and fluid circulation via a sheet that is stretching in Newtonian and non-Newtonian fluids under the effect of electric and magnetic fields, variable thermal boundary conditions, and power law change of the strengthening exercises velocity are currently explored.

The literature on nanofluids has been reviewed by Trisaksri and ongwises [17], Wang and Mujumdar [18], and Kakac and Pramuanjaroenkij [4], Boungiorno [3] among several others. These reviews analyse in detail the research on convective transport in nanofluids and improved an analytical model for convective transport in nanofluids including the Brownian diffusion and thermophoresis.

To estimate It is vital to account for the fluctuation in permeability with warmth when calculating the rate of heat transfer. The thermal boundary layer has a wide range of viscosity. Several scholars have studied flows with temperature dependent viscosity across many geometries and circumstances by (Rahman and Eitayab [11],Mukhopadhyya and Layek [8], Ali [2], Prasad *et al*. [10], Alam *et al*. [1]). They found that in the presence of variable viscosity the flow characteristics change appreciably compared with the constant viscosity case. The hydromagnetic flow with variable viscosity and thermal radiation have been dealt by Makinde[6,7] and Salem [13]. Sreedevi et al [15, 16] investigated the influence of radiation absorption and variable viscosity on hydromagnetic convective heat and mass transfer flow across a stretched sheet using Cuo-water nanofluid.

The effect of Newtonian cooling and activation energy on convective heat transfer flow of nanofluid past as stretching with variable viscosity and partial slip. Nonlinear governing equations have been solved numerically by Runge-Kutta-Fehlberg method along with shooting technique. The effect of various parameters on the flow variables have been discussed in different graphs.

Nomenclatures

u,v,w	velocity components
x,y,z	coordinates
D_m	diffusivity
K_T	thermal diffusion ratio
C_s	concentration susceptibility
C_p	specific heat at constant pressure
$\sigma^•$	Stefan-Boltzmann constant

β_R	mean absorption coefficient
T_m	mean fluid temperature
Ea	activation energy coefficient
f	dimensionless stream function
h	similarity space variable
θ	dimensionless temperature
ϕ	concentration
C_f	skin-friction number
Nu	Nusselt number
Sh	Sherwood number
γ>0	degenerating chemical reaction
γ<0	generating chemical reaction
f'	primary velocity
g	secondary velocity
θ	temperature
ϕ	nano particle concentration

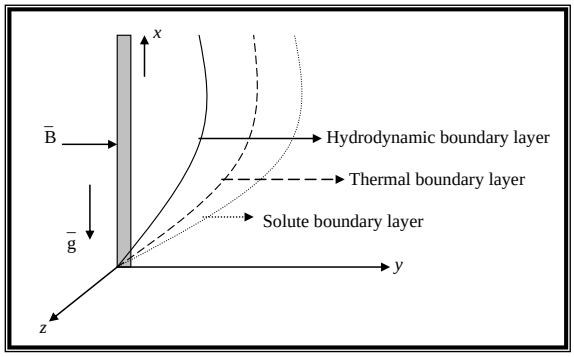

Fig.1 : Physical System and Geometry of the Problem

2. MATHEMATICAL ANALYSIS

The constant free-convective flow, warmth, and the transfer of mass of a nanofluid across a sheet that has been stretched are all taken into account. The sheet is stretched at a rate proportionate to its angle to the set basis O (Fig. 1). The flow becomes three-dimensional. Let T_w, C_w be wall temperature(θ) and species concentration(ϕ) and T_∞ and C_∞ be the fixed values far away from the sheet.

It is believed that fluid viscosity μ varies as a double of an exponential function of ambient temperature obtained from

$$\frac{1}{\mu} = \frac{1}{\mu_\infty}[1+\gamma_0(T-T_\infty)] \quad (1)$$

$$\frac{1}{\mu_\infty} = a(T-T_\infty) \quad (2)$$

where $a = \frac{\gamma_0}{\mu_\infty}$ and $T_r = T_\infty - \frac{1}{\gamma_0}$

Each a and T_r are parameters in the preceding equation, and their quantities are determined by the fluid's thermal properties. In all likelihood, $a > 0$ represents liquids, although $a<0$ represents gases.

The boundary layer free-convection flow with mass transfer and generalised Ohm's law with Hall current effect under Boussinesq and Rosseland approximations is controlled by the following collection of formulas using the aforementioned beliefs:

$$\frac{\partial u}{\partial x} + \frac{\partial v}{\partial y} = 0 \quad (3)$$

$$\rho_{nf}\left(u\frac{\partial u}{\partial x} + v\frac{\partial u}{\partial y}\right) = \mu_{nf}\frac{\partial^2 u}{\partial y^2} + (\rho\beta)_{nf} \left| g(T-T_\infty) - \frac{\sigma_{nf}B_0^2}{1+m^2}(u+mw) \right. \quad (4)$$

$$\rho_{nf}\left(u\frac{\partial w}{\partial x} + v\frac{\partial w}{\partial y}\right) = \mu_{nf}\frac{\partial^2 u}{\partial y^2} + \frac{\sigma_{nf}B_0^2}{1+m^2}(mu-w) \quad (5)$$

$$(\rho C_p)(u\frac{\partial T}{\partial x} + v\frac{\partial T}{\partial y}) = (k_f + \frac{16\sigma^{\bullet}T_\infty^3}{3\beta_R})\frac{\partial T^2}{\partial y^2} + \left| + \tau\{D_B(\frac{\partial T}{\partial y}\frac{\partial C}{\partial y} + \frac{D_T}{T_0}(\frac{\partial T}{\partial y})^2) \right. \quad (6)$$

$$u\frac{\partial C}{\partial x} + v\frac{\partial C}{\partial y} = D_m\frac{\partial^2 C}{\partial y^2} - k_0(C-C_\infty) \left| (\frac{T}{T_\infty})^n Exp(-\frac{E_a}{KT}) + \frac{D_m K_T}{T_m}\frac{\partial^2 T}{\partial y^2} \right. \quad (7)$$

where the above component and parameters are shown in Nomenclature. Can be written the current issues of the boundary conditions were

$$u=bx \quad ,v=w=0, -k_{nf}\frac{\partial T}{\partial y} = h_1^{'}(T_w - T), C=C_w \quad (8)$$

$$u \to 0,\ w \to 0,\ T \to T_\infty,\ C \to C_\infty \text{ at } y \to \infty \quad (9)$$

where b (> 0) denotes the sheet's stretching rate. In Eq.(8), the governing constraints on velocity are provided that there is no slip at the outermost point y = 0, but the criteria for the conditions governing the boundaries on velocity at y→ ∞ derive from the fact that there is no flow far away from the stretched surface. The subsequent transformations are call on observe the flow regime adjacent to the sheet,

$$u = bxf'(\eta); v = -\sqrt{bv}\,f(\eta); w = bxg(\eta);$$

$$\eta = \sqrt{\frac{b}{v}}\,y; \theta(\eta) = \frac{T-T_\infty}{T_w-T_\infty}; \phi = \frac{C-C_\infty}{C_w-C_\infty} \quad (13)$$

Where parameter are shown Nomenclatures. The continuity Eq. (3) is contented by u and v clear in Eq. (9), use as a replacement of Eq. (10) the Eqs. (4)-(7) diminish to

$$(\frac{\theta-\theta_r}{\theta_r})(f' - f\,f'') + f''' - (\frac{\theta'}{\theta-\theta_r})f'' - (\frac{\theta-\theta_r}{\theta_r}) \quad (14)$$
$$G(\theta+N\varphi) + M^2((\frac{\theta'-\theta_r}{\theta_r})(\frac{f'+mg}{1+m^2}) = 0$$

$$\left.\begin{aligned}(\frac{\theta-\theta_r}{\theta_r})(f'g-fg')+g''-(\frac{\theta'}{\theta-\theta_r})g'-\\ -M^2(\frac{\theta-\theta_r}{\theta_r})(\frac{mf'+g}{1+m^2})=0\end{aligned}\right| \quad (15)$$

$$(1+\frac{4Rd}{3})\theta''+Nb(\theta'C')+Nt(\theta')^2+Q\theta=0 \quad (16)$$

$$C''-Sc(fC'-\gamma C)+(\frac{Nt}{Nb})\theta''-\gamma(1+n\delta\theta)\,\mathrm{E}\,xp(-\frac{E_1}{1+\delta\theta})=0 \quad (17)$$

The boundary conditions of transformed below

$f'(\eta)=1, f(\eta)=0, g(\eta)=0, \theta'(0)=-h_1(1-\theta(0))$,

C (η)=1 at η=0 (18)

$f'(\eta)\to 0$, $g(\eta)\to 0$, $\theta(\eta)\to 0$, C (η) → 0 at η → ∞ (19)

where the prime value represents the differentiation exclusively with regard to η the dimensionless parameters in the Eqs. (14) through (17) are characterised as

$\theta_r=\frac{T_r-T_\infty}{T_w-T_\infty}=-\left[\frac{1}{\gamma_0(T_w-T_\infty)}\right]$, $M=\frac{\sigma B_0^2}{P_\infty b}$,

$P_r=\frac{\rho C_p \nu}{k}$, $\gamma=\frac{k_0}{b}(C_w-C_\infty)$, $G=\frac{g_0\beta_T(T_w-T_\infty)}{b^2x}$,

$N=\frac{\beta_C(C_w-C_\infty)}{\beta_T(T_w-T_\infty)}$, $Nr=\frac{kk_0}{4T_\infty{}^3\sigma^*}$, $Le=\frac{\mu}{\rho_\infty D}$,

$Rd=\frac{4\sigma^{\bullet}T_\infty^3}{3\beta_R k_f}$, $Nb=\frac{\tau D_B(C_w-C_\infty)}{k_f}$, $Nt=\frac{\tau D_T(T_w-T_\infty)}{T_\infty k_f}$,

$h_1=\frac{h_1'}{k_f}\sqrt{\frac{b}{\nu}}$, $E1=\frac{E_n}{kT_0}$, $\theta w=\frac{T}{T_w}, \delta=\theta_w-1$ are the viscosity, magnetic, Prandtl number, non-dimensional chemical reaction, local Grashof number, Buoyancy ratio, thermal radiation parameter, Schmidt number, radiation parameter. Brownian motion parameter, thermophoresis parameter, convective heat parameter, Activation energy parameter, temperature difference ratio.

3. METHOD OF SOLUTION

The equations **(14)-(17)along with the** boundary conditions (18&19) constitute a set of nonlinear non-homogeneous differential equations for which closede form solution is out of reach. Hence solved numerically using a shooting technique. The details of the method can be found in Cebeci and Bradshaw (3a). This method involves, transforming the equation into a set of initial value problems (IVP) which contain unknown initial values that need to be determined by first guessing, after which the Runge-Kutta iteration scheme is employed to integrate the set of IVPs until the given boundary conditions are satisfied.

4. SKIN FRICTION, NUSSELT NUMBER AND SHERWOOD NUMBER

Skin friction (C_f), Nusselt (Nu) and Sherwood (Sh) numbers are defined by

$$C_f=\frac{\tau_w}{\mu bx\sqrt{\frac{b}{\nu}}}=f''(0) \quad (20)$$

Where

$$\tau_w=\mu\left(\frac{\partial T}{\partial y}\right)_{y=0}=\mu bx\sqrt{\tfrac{b}{\nu}}f''(0), Nu=\frac{\dot{q}_w}{k\sqrt{\frac{b}{\nu}}(T_w-T_\infty)} \quad (21)$$

where $q_w=-k\left(\frac{\partial T}{\partial y}\right)_{y=0}=-k_f\sqrt{\frac{b}{\nu}}(T_w-T_\infty)\theta'(0)$ and

$$Sh=\frac{m_w}{D_B\sqrt{\frac{b}{\nu}}(C_w-C_\infty)}=-\phi'(0) \quad (22)$$

where $m_w=-D_B\left(\frac{\partial \phi}{\partial y}\right)_{y=0}=-D_B\sqrt{\frac{b}{\nu}}(C_w-C_\infty)\phi'(0)$

5. COMPARISON

The findings of this work correlate to the findings of prior to articles released by Shit et al. [14] and Rahman et al. [12], as shown in Tables 1a and 1b, and the results are in good agreement (E1=0, δ=0).

Table 1a. Shit et al. [14], Nu and Sh at η=0 of Comparison

M	Nr	Γ	θr	Shit et al.[14]Results		Present Results	
				Nu(0)	Sh(0)	Nu(0)	Sh(0)
0.5	1	0.5	-2	-0.6911	0.6267	-0.6912	0.6277
1.5	1	0.5	-2	-0.6973	0.6544	-0.6977	0.6550
0.5	3	0.5	-2	-12.3749	0.9279	-12.3752	0.9282
0.5	1	1.5	-2	-0.6952	1.0957	-0.6955	1.0955
0.5	1	-0.5	-2	-0.6964	0.4899	-0.6966	0.4901
0.5	1	-1.5	-2	-0.6962	0.4247	-0.6969	0.4252
0.5	1	0.5	-4	-0.6976	0.6256	-0.6979	0.6259

Table 1b. Rahman et al. [12], Nu and Sh at η=0 of Comparison through Pr=0.71, m= Nb=Nt= γ= 0,E1=0,=0 for different values of θr

Different Values of θr	Rahman et al. [12] Results		Present Results	
	Nu(0)	Sh(0)	Nu(0)	Sh(0)
-2	-0.37865	4.80535	-0.37842	4.80539
-4	-0.30537	4.54269	-0.30523	4.54275
2	0.24825	4.48563	0.24812	4.48565
4	0.23878	4.33566	0.23882	4.33572

6. FINDINGS

The non-linear governing equations have been solved by applying the fourth order Runge-Kutta shooting method. Using the *MATHEMATICS* the finding represents in graphs(Figs.2a,

2b, 3a, 3b, 4a, 4b, 5a, 5b, 6a, 6b, 7a and 7b) which in *f'* and *g*, θ and ϕ through computed of different parameters.

The primary and secondary velocities(*f ′*, *g*) rise with an increase in the Hall parameter(m),emission constraint (*Nr*), Brownian movement constraint (*Nb)*, Radiation parameter (Rd), convective heat transfer constant(h1), activation energy parameter (E1). The growth in the Hall parameter, emission constraint, Brownian movement constraint, radiation parameter, convective heat transfer constant, activation energy constraint upsurges the width of the boundary layer of the conduit walls, which bigger the *f ′*, *g* (figs.2a, 2b, 3a, 3b, 5a, 5b, 6a, 6b, 7a, 7b). In the case of an increase in the thermo-phoresis constraint (*Nt*),temperature difference ratio(δ) decays the velocities(figs.3a,3b,7a,7b).

Increase in variable viscosity constraint(θr) enhances *f ′* and depreciates *g* (figs.5a,5b). *f ′* diminishes and *g* upsurges in γ>0 while for γ<0, an opposite behaviour is noticed in the velocities(figs.4a,4b).

It is noticed that θ and ϕ decrease with increase in Hall parameter(m), emission constratint(Nr), radiation constraint (Rd), variable viscosity constraint(θr). (figs. 2c, 2d, 5c, 5d). Increase in Brownian movement constraint enhances both θ and ϕ in the flow region (figs.3c,3d). Increase in thermophoresis constraint(Nt), convective heat transfer constraint(h1), temperature difference ratio(δ) leads to a rise in θ and fall in ϕ (figs.3c, 3d, 6c, 6d, 7c, 7d). θ and ϕ depreciate in γ>0 and grow in γ<0 (figs.4c,4d). Higher the activation energy constraint (E1) smaller the θ and larger the ϕ in the flow region (figs,7c, 7d).

The variation of Skin friction(C_f), rate of heat and mass transfer(Nu & Sh) in table.2 are exhibited. An increase in *m* parameter grows Cfx,Cfz,Nu and Sh at η=0. When the molecular buoyancy force dominates over the thermal buoyancy force (Cfz),Nu and Sh grow ,Cfx decays at the wall when the forces are in the same direction. With reference to the radiation parameter(Rd) it is found that an increase in Rd decays the skin friction coefficient(Cfx) and enhances Cfz,Nu,Sh at η=0. An upsurge in the viscosity parameter (θr) grows Cfx and decays (Cfz), Nu,Sh at η=0. Nu & Sh upsurges in γ<0 while in γ>0 an opposite result is noticed. An increase in Brownian motion parameter(Nb)larger (Cfz),smaller (Cfx),Nu and Sh at the wall. Higher thermophoresis parameter(Nt) larger skin friction (Cfx),rate of heat and mass transfer while smaller (Cfz) at η=0.Higher the convective heat transfer constant(h1) smaller Cfx,Nu and larger Cfz,Sh on η=0. Increase in activation energy (E1)leads to a rise in Cfz,Nu and fall in Cfx,Sh on η=0 while an opposite behaviour is noticed with temperature difference ratio(δ).

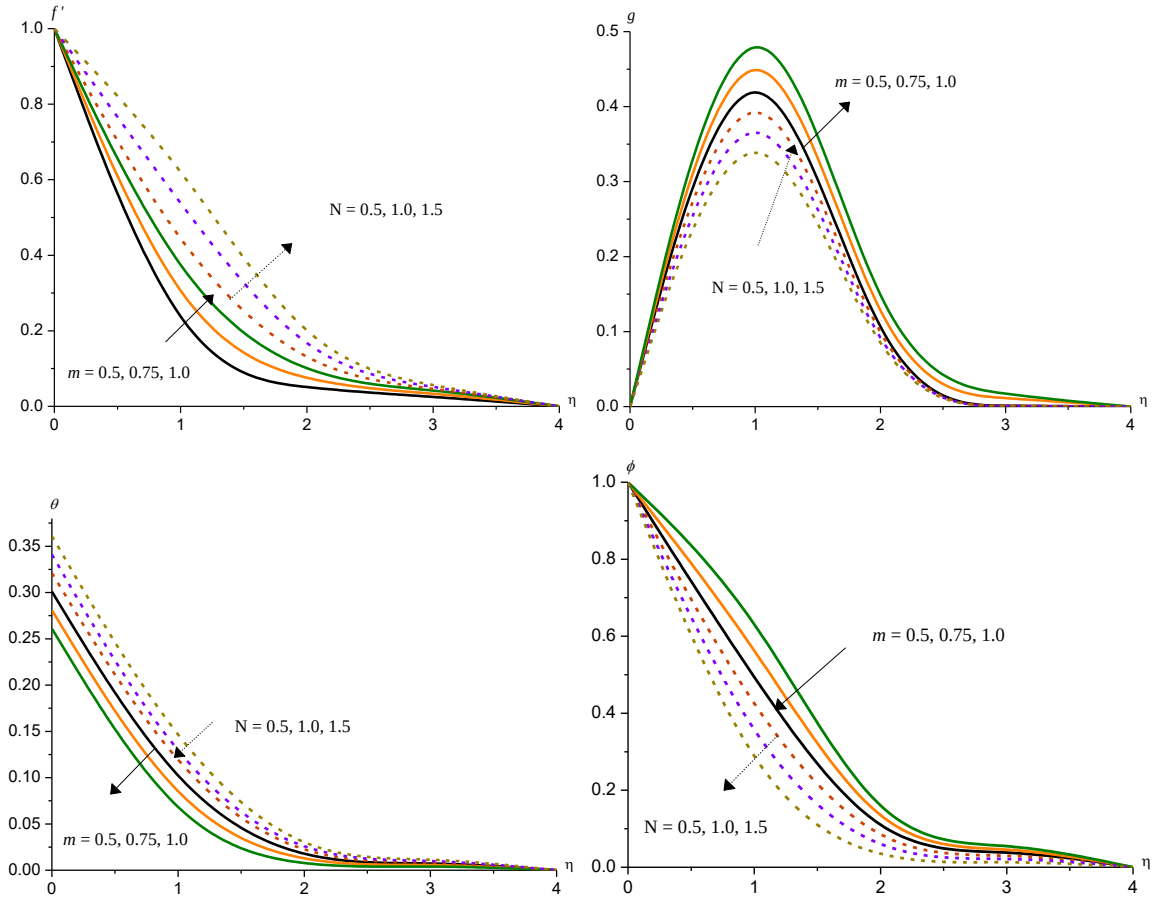

Fig.2: Variation of [a] axial velocity(*f ′*), [b] Secondary velocity(*g*), [c] Temperature(θ), [d] Nano-Concentration(ϕ) with *m* and *N* G=2, M=0.5, Rd=0.5, θr=-2, γ=0.5, Nb=0.1,m Nt=0.1, h1=0.1, E1=0.1, δ=0.2, Pr=0.71, Le=2

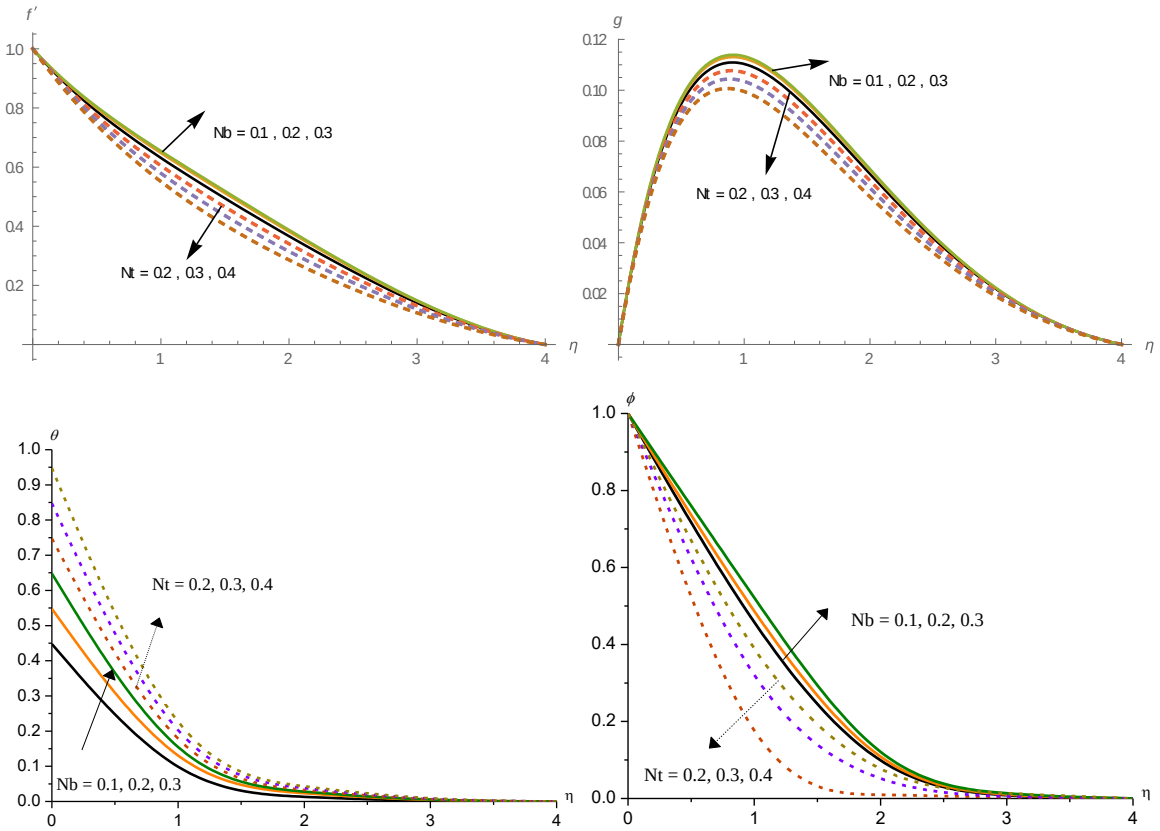

Fig.3: Variation of [a] axial velocity(*f ′*), [b] Secondary velocity(*g*), [c] Temperature(θ), [d] Nano-Concentration(ϕ) with Nb and Nt

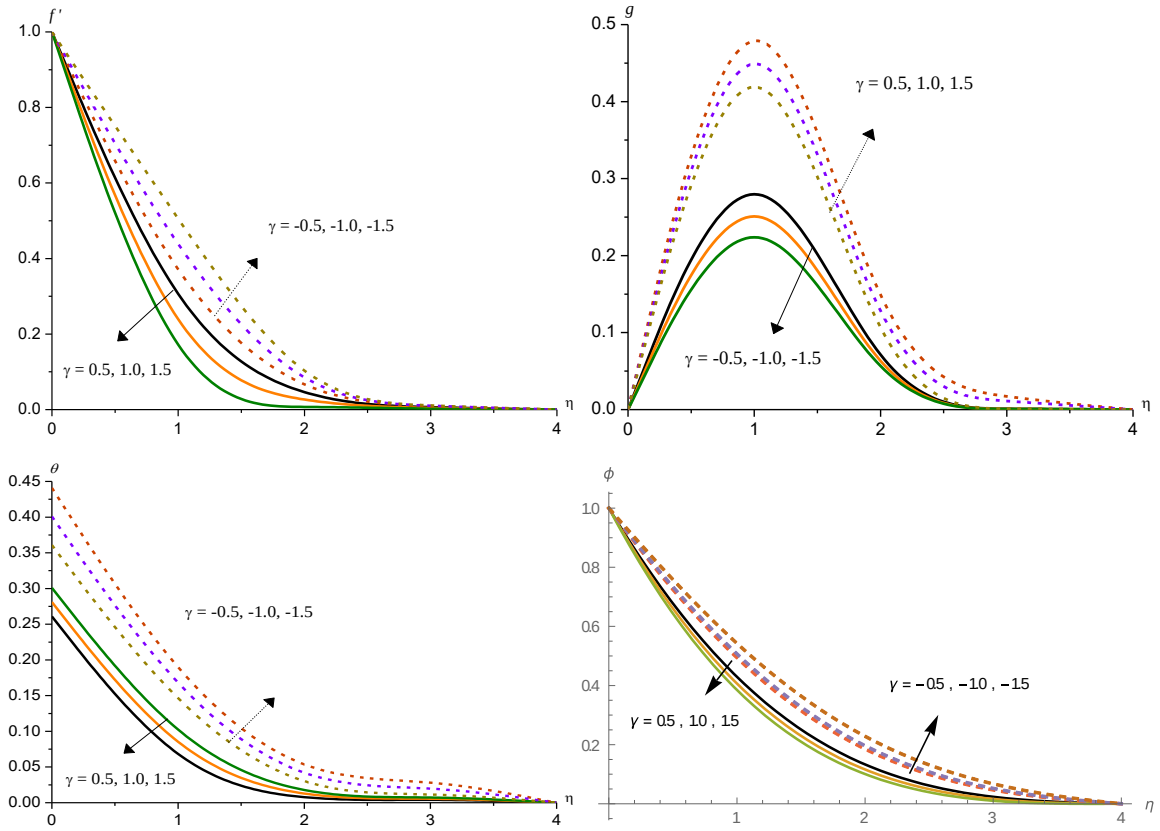

Fig.4: Variation of [a] axial velocity(*f ′*), [b] Secondary velocity(*g*), [c] Temperature(θ), [d] Nano-Concentration(ϕ) with γ

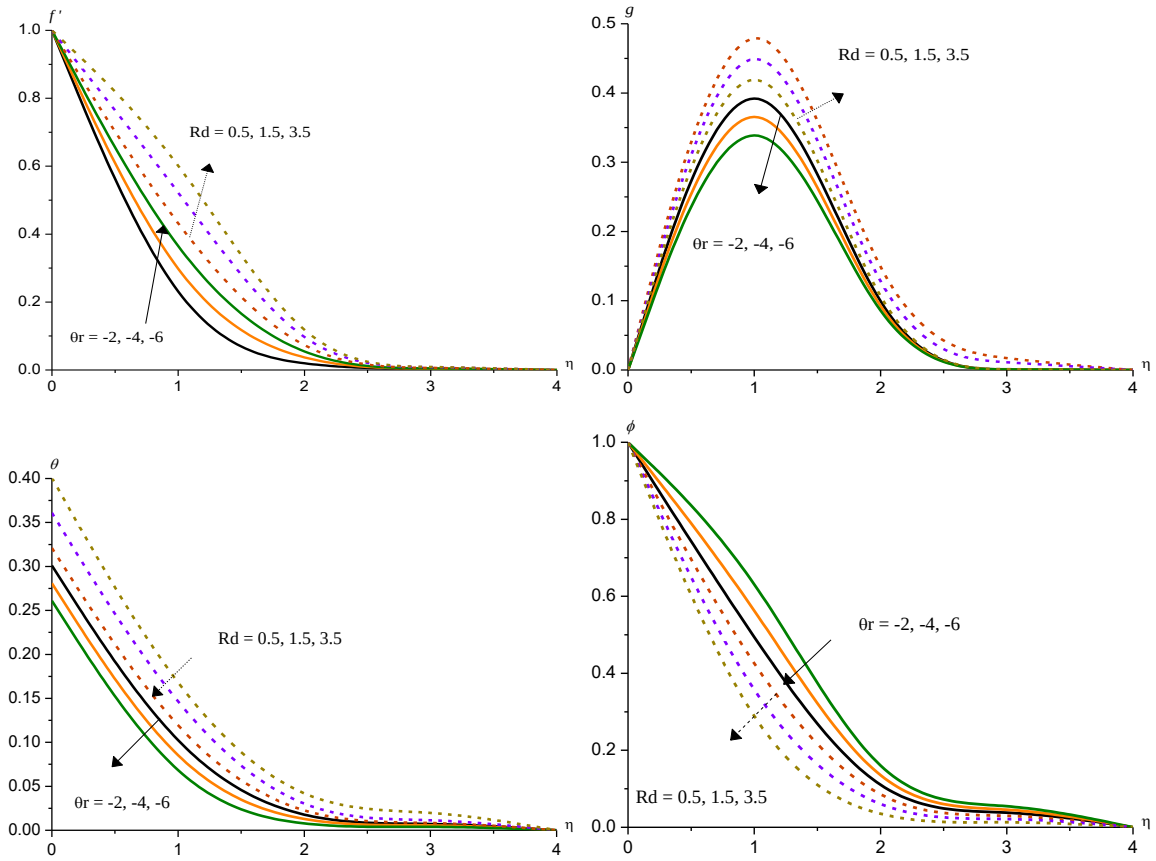

Fig.5: Variation of [a] axial velocity(f'), [b] Secondary velocity(g), [c] Temperature(θ), [d] Nano-Concentration(ϕ) with θr and Rd

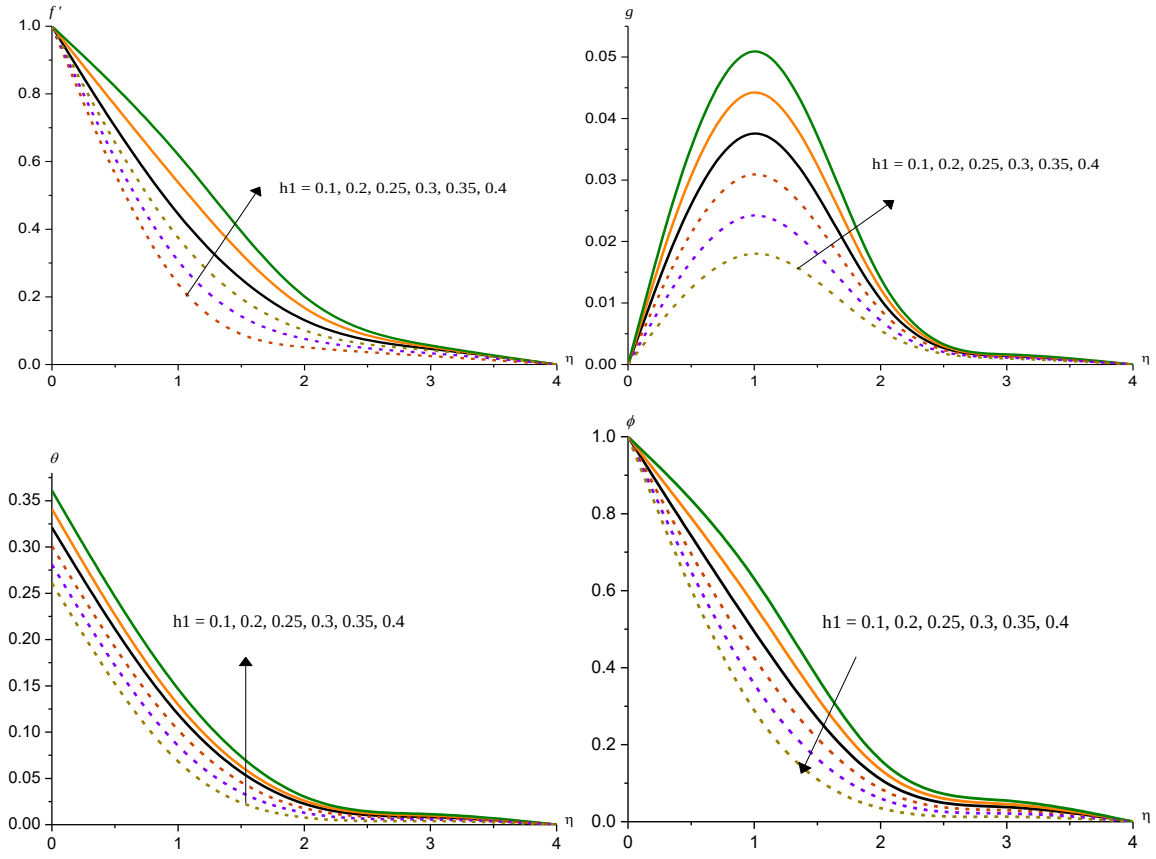

Fig.6: Variation of [a] axial velocity(f'), [b] Secondary velocity(g), [c] Temperature(θ), [d] Nano-Concentration(ϕ) with h1

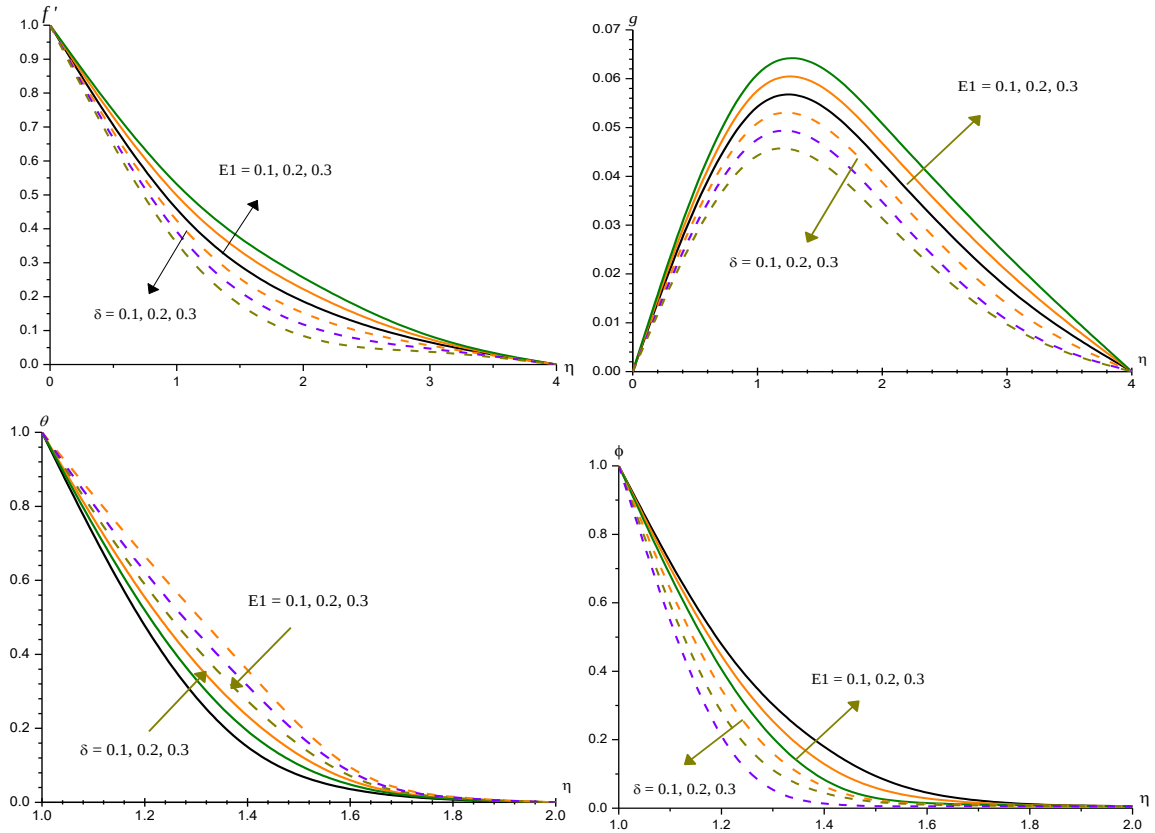

Fig.7: Variation of [a] axial velocity(f'), [b] Secondary velocity(g), [c] Temperature(θ), [d] Nano-Concentration(ϕ) with E1 and δ

Table – 2 Skin Friction ($Cf_{x,z}$), Nusslet number (Nu) and Sherwood Number (Sh) at η = 0

Parameter		$Cf_x(0)$	$Cf_z(0)$	Nu(0)	Sh(0)	**Parameter**		$Cf_x(0)$	$Cf_z(0)$	Nu(0)	Sh(0)
m	0.5	-0.355923	0.303329	0.0687655	0.697745	Nb	0.1	-0.513033	0.313112	0.0690176	0.721081
	1.0	-0.421249	0.398547	0.0691822	0.723509		0.2	-0.487727	0.316919	-0.0117127	0.609601
	1,5	-0.449063	0.433889	0.0673211	0.725529		0.3	0.475515	0.318827	-0.0087193	0.577151
N	0.5	-0.431255	0.317184	0.0691522	0.722924	Nt	0.1	-0.475515	0.308686	-0.0123103	0.968173
	1.0	-0.323128	0.322435	0.0693303	0.725327		0.2	-0.544435	0.304159	-0.0303323	1.200982
	1.5	-0.269442	0.324989	0.0694187	0.726506		0.3	-0.574911	0.299056	-0.0489186	1.442032
Rd	0.5	-0.317396	0.291537	-0.049311	0.826508	h1	0.1	-0.514672	0.312827	0.0692503	0.720511
	1.5	-0.220955	0.345041	-0.119867	0.974017		0.2	-0.513808	0.312977	0.0691278	0.720812
	3.5	-0.143496	0.389121	-0.415966	1.578952		0.25	-0.513033	0.313112	0.0690176	0.721081
θr	-2	-0.355923	0.303329	0.0687655	0.747745		0.3	-0.512811	0.313114	0.0689858	0.721159
	-4	-0.503225	0.300298	0.0690314	0.721304		0.35	-0.512608	0.313186	0.0689569	0.721229
	-6	-0.529641	0.263505	0.0690415	0.721867		0.4	-0.512116	0.313271	0.0688866	0.721433
E1	0.1	-1.00519	0.218212	0.135731	0.669726	γ	0.5	-0.355923	0.303329	0.0687655	0.717745
	0.2	-0.99951	0.219152	0.135744	0.630935		1.0	-0.518322	0.312482	0.0718984	0.766751
	0.3	-0.99455	0.219988	0.135748	0.597914		1.5	-0.524017	0.321814	0.0751133	0.817945
δ	0.2	-1.01047	0.217355	0.135722	0.707252		-0.5	-0.496048	0.315222	0.0604131	0.584771
	0.3	-1.01545	0.216633	0.135715	0.740324		-1.0	-0.492872	0.315625	0.0589067	0.560792
	0.4	-1.01927	0.215965	0.135709	0.772483		-1.5	-0.484015	0.316772	0.0548573	0.495979

7. CONCLUSIONS

The summaries and conclusion are stated that:

- The Hall current/buoyancy ratio(N), axial velocity, cross flow velocity enhance, temperature and nanoconcentration reduces. With increase in m/N, skin friction coefficient Cfz,Nu and Sh enhance ,while Cfx grows with m and decays with N on the wall.
- Brownian motion (Nb) and thermophoresis (Nt) has the effect of increasing the temperature in the flow region. Nu and Sh grow with Nt ,decay with Nb on η=0.
- The axial velocity increases, temperature and nanoconcentration depreciate in the flow region with increase in the radiation parameter(Rd) and viscosity parameter (θr).Cross flow velocity grows with Rd and decays with θr.Cfz, Nu, Sh increase with θr and reduce with Rd and .Cfx reduces with Rd and enhances with θr.

- The velocities ,temperature grow, nanoconcentration reduces with rising values of convective heat transfer constant(h1).Cfx, Nu reduce, Cfz, Sh increase with increase in h1 on η=0.
- The velocities, nanoconcentration augment, temperature depreciates with activation energy parameter(E1) while an opposite behaviour is observed with δ.Cfx, Sh decay, Cfz, Nu grow with E1 on η=0.

8. REFERENCES

[1] Alam MS, Rahman MM, Sattar MA. Transient magnetohydrodynamic free convective heat and mass transfer flow with thermophoresis past a radiate inclined permeable plate in the presence of variable chemical reaction and temperature dependent viscosity. Nonlinear Anal. Modell. Control, V.14(1), pp:3-20(2009).

[2] Ali ME. The effect of variable viscosity on mixed convection heat transfer along a vertical moving surface. Int. J. Therm. Sci., V.45(1), pp:60-9 (2006).

[3] Buongiorno. J (2006): Convective transport in nanofluids," ASME J Heat Tran vol.128, pp:240–250.

[4] [3a] Cebeci T, Bradshaw P(1988):Physical and computational aspects of convective heat transfer. New York: Springer.

[5] Kakac S. *et al.*Review of convective heat transfer enhancement with nanofluids Int. J. Heat Mass Transf. (2009)

[6] Makinde O.D., Aziz A., Boundary layer flow of a nanofluid past a stretching sheet with a convective boundary condition, International Journal of Thermal Sciences, 50 (2011) 1326e1332, doi:10.1016/ j.ijthermalsci.2011.02.019

[7] Makinde OD. Laminar falling liquid film with variable viscosity along an inclined heated plate. Appl Math Comput V.175(1), pp:80-8(2006).

[8] Makinde,O.D:Second law analysis for variable viscosity hydromagnetic boundary layer flow with thermal radiation and Newtonian heating.,Entrophy V.13,pp.1446-1464(2011)

[9] Mukhopadhyay S, Layek GC. Effects of thermal radiation and variable fluid viscosity on free convective flow and heat transfer past a porous stretching surface. Int J Heat Mass Transf, V.51(9-10), pp:2167-78(2008).

[10] Oztop. H. F and Abu-Nada. E (2008): Numerical study of natural convection in partially heated rectangular enclosures filled with nanofluids.,Int.J.Heat and Fluid Flow., V.29,pp.1326-1336.

[11] Prasad KV, Vajravelu K, Datti PS. The effects of variable fluid properties on the hydro-magnetic flow and heat transfer over a non-linearly stretching sheet. Int J Therm Sci, V.49(3), pp:603-10(2010).

[12] Rahman,M and Salahuddin,K.M:Study of hydromagnetic heat and mass Transfer flow over an inclined heated surface with variable viscosity and electric conductivity., Commun. Nonlinear Sci.Numer.Simulat,V.15,pp.2073-2085 (2010)

[13] Rahman,M and Salahuddin,K.M:Study of hydromagnetic heat and mass Transfer flow over an inclined heated surface with variable viscosity and electric conductivity., Commun. Nonlinear Sci.Numer.Simulat,V.15,pp.2073-2085(2010)

[14] Salem AM. Variable viscosity and thermal conductivity effects on MHD flow and heat transfer in viscoelastic fluid over a stretching sheet. Phys Lett A; V.369(4), pp:315-22(2007).

[15] Shit GC and Haldar R. Combined effects of Thermal Radiation and Hall Current on MHD Free-Convective Flow and Mass Transfer over a Stretching Sheet with Variable Viscosity. J Applied Fluid Mechanics; V.5, pp: 113-21 (2012).

[16] Sreedevi,G, Prasada Rao,D.R.V and Ali J Chamka: Convective heat transfer of a nano fluid over a stretching sheet with variable viscosity and hall effect, Journal of Mathematical fluid mechanics, Vol.3, pp.1023-1033, (2020).

[17] Sreedevi,G,Raghavenra Rao,R,Prasada Rao,D.R.V and Ali J Chamka:Influence of radiation absorption and Hall current effects on convective heart and mass transfer flow past a stretching sheet, Accepted for publication,Ain shams Journal(2015).

[18] Trisaksri V. *et al.* Critical review of heat transfer characteristics of nanofluids Renew. Sust. Energ. Rev.(2007)

[19] Wang X.-Q. *et al.*Heat transfer characteristics of nanofluids: a review nt. J. Therm. Sci. 2007).

[20] Watanabe T, Pop I. Hall effects on magneto-hydrodynamic boundary layer flow over a continuous moving flat plate. Acta Mechanica; V.108, pp:35-47 (1995).